Proceedings of the Thirty-fifth (2025) International Ocean and Polar Engineering Conference **www.isope.org**
Seoul/Goyang, Korea, June 1-6, 2025

ISBN 978-1-880653-74-6; ISSN 1098-6189

Enhancing the Hydrodynamic Modeling of Spar-Type Floating Offshore Wind Turbines: Incorporating Vortex-Induced Vibrations in OpenFAST

Taeksang Kim[1], Jeongbin Park[2], Seymour M.J. Spence[1], Yulin Pan[2], Ayumi Fujisaki-Manome[3], Jeremy David Bricker[1,4]*
[1] Department of Civil and Environmental Engineering, University of Michigan, Ann Arbor, MI, USA.
[2] Department of Naval Architecture and Marine Engineering, University of Michigan, Ann Arbor, MI, USA.
[3] Cooperative Institute for Great Lakes Research, University of Michigan, Ann Arbor, MI, USA.
[4] Faculty of Civil Engineering & Geosciences, Department of Hydraulic Engineering, Delft University of Technology, 2600 GA Delft, The Netherlands
[*]Corresponding author

ABSTRACT

Floating Offshore Wind Turbines (FOWTs) operate under complex environmental conditions, where unsteady hydrodynamic forces such as vortex-induced vibrations (VIV) can significantly influence structural response. However, conventional modeling approaches often neglect VIV effects, leading to underestimation of platform motion and hydrodynamic loading. This study incorporates a VIV-induced lift force model into the Morison equation framework within OpenFAST to assess its impact on the dynamic behavior of a spar-type FOWT under steady current conditions. Two simulation cases are compared: one assuming a stationary platform and the other allowing for platform motion through relative velocity coupling. Results show that VIV introduces multi-frequency oscillations in both hydrodynamic force and platform sway response, with amplitudes increasing with current speed. These findings focus on the importance of including VIV effects in hydrodynamic models for accurate prediction of FOWT behavior.

KEY WORDS: Floating offshore wind turbine (FOWT); vortex-induced vibrations (VIV); hydrodynamic modeling; Morison equation; OpenFAST.

INTRODUCTION

Floating Offshore Wind Turbines (FOWTs) are a key technology for offshore wind energy, allowing power generation in deep waters where fixed-bottom turbines are impractical. As global interest in renewable energy grows, FOWTs provide a promising solution by harnessing stronger and more consistent offshore winds. However, their floating nature introduces complex engineering challenges due to interactions between aerodynamic, hydrodynamic, and structural forces, as well as mooring dynamics. FOWTs continuously respond to wind, waves, and currents, requiring advanced numerical modeling to ensure stability, efficiency, and durability (Jonkman and Buhl, 2005).

Among the most widely used simulation tools for FOWTs is OpenFAST, developed by the National Renewable Energy Laboratory (NREL). OpenFAST integrates multiple modules, including AeroDyn (aerodynamics), HydroDyn (hydrodynamics), ElastoDyn (structural response), and MoorDyn (mooring dynamics) (Jonkman and Buhl, 2005; Jonkman, 2009). HydroDyn, responsible for hydrodynamic force calculations, traditionally combines potential flow theory with Morison's equation, where the former accounts for wave radiation and diffraction forces, while the latter estimates viscous drag and inertia on slender structures (Morison et al., 1950). While this hybrid approach has been effective in many offshore applications, it does not inherently include vortex-induced vibrations (VIV), which play a crucial role in FOWTs.

VIV occurs when periodic vortex shedding generates oscillatory forces on cylindrical structures, potentially leading to resonance, fatigue damage, and altered dynamic responses. This phenomenon is particularly relevant for mooring lines, towers, and other cylindrical components, where unaccounted oscillations can accelerate fatigue failure. Experimental studies have shown that ignoring VIV underestimates fatigue loads, which could compromise long-term structural integrity (Sumer, 2006). Numerical studies further confirm the importance of incorporating VIV in hydrodynamic models for accurate behavior prediction of offshore structures (Facchinetti et al., 2004; Gabbai and Benaroya, 2005). While OpenFAST's HydroDyn module applies Morison's equation for force estimation, it currently lacks a VIV model, limiting its ability to capture all hydrodynamic forces acting on FOWTs (Williamson and Govardhan, 2004). To address this limitation, this study integrates VIV modeling into OpenFAST's HydroDyn module using a Morison equation-only approach, rather than a hybrid model that includes potential flow theory. Potential flow theory primarily accounts for wave radiation and diffraction under the assumption of inviscid flow, whereas VIV is a viscous flow phenomenon caused by vortex shedding. Since potential flow theory alone cannot accurately capture VIV effects, isolating VIV within the Morison framework ensures that wave-induced and vortex-induced forces do not interfere. This approach provides a focused and computationally efficient method for modeling VIV forces, allowing for validation before incorporating more complex hydrodynamic interactions.

Hydrodynamic modeling of FOWTs has been an area of active research,

with various techniques developed to improve force estimation beyond traditional Morison-based models. Computational Fluid Dynamics (CFD) has been widely used to capture turbulence, wake effects, and vortex shedding (Tran and Kim, 2015, 2016). However, full-scale CFD simulations remain computationally expensive, making them impractical for large-scale FOWT analyses (Zhang et al., 2024). To address this limitation, hybrid models combining potential flow theory with viscous corrections have been introduced to improve hydrodynamic force predictions while maintaining computational efficiency (Zhong et al., 2022). Another approach involves strip theory-based methods, where localized CFD solutions are applied along the structure to better capture VIV effects (Chen et al., 2019).

The standard Morison equation in HydroDyn does not account for oscillatory lift forces induced by vortex shedding, leading to inaccuracies in predicting FOWT dynamics. To address this limitation, this study incorporates modifications based on experimentally developed nonlinear models for vortex shedding forces acting on oscillating cylinders (Blevins, 2009). These modifications introduce additional force terms derived from VIV models, allowing HydroDyn to more accurately capture unsteady hydrodynamic loads, particularly in sway, roll, and yaw, where VIV effects are most significant. Given the effectiveness of VIV-inclusive models in offshore structure analyses, integrating these methods into HydroDyn is a crucial step toward improving FOWT simulations.

This study develops a modified OpenFAST framework that incorporates VIV effects into HydroDyn to improve FOWT hydrodynamic modeling. Using the NREL 5MW FOWT with a spar-type platform, the modified Morison equation accounts for vortex shedding forces. The computational setup prescribes steady current-only boundary conditions, systematically varying current speed to investigate the platform response under different flow regimes. By excluding waves and wind, the analysis focuses on the hydrodynamic impact of current-induced VIV, enabling a clearer understanding of its role in platform dynamics.

METHODOLOGY

Wind Turbine Model Properties

5MW wind turbine. This study employs a numerical simulation of a 5MW floating offshore wind turbine (FOWT) to evaluate the impact of VIV on platform motion. The simulation follows the NREL 5MW reference wind turbine specifications (Jonkman et al., 2009). As illustrated in Fig. 1, the floating system consists of a spar-type platform, mooring lines, and a tower, with the rotor blades included in the model. While AeroDyn is active, this study does not account for VIV-induced aerodynamic effects, meaning that VIV-related unsteady aerodynamic forces, such as those caused by the tower shadow effect, are not included. The primary focus remains on hydrodynamic interactions and how VIV alters the structural response of the FOWT through forces acting on the platform, tower, and mooring lines.

Spar type floating platform. The OC3 spar-type platform (Jonkman, 2010) is selected in this study. The platform extends 120 m below the still water level (SWL) with a diameter of 6.5 m above taper and 9.4 m below taper. The total platform mass, including ballast, is 7,466,330 kg, with a center of mass located 89.92 m below SWL. The platform's roll/pitch inertia is 4.23×10^9 kg·m², and the yaw inertia is 1.64×10^8 kg·m².

Tower. The wind turbine tower has a total height of 87.6 m, with the base positioned 10 m above SWL. The tower diameter tapers from 6.5 m at the base to 3.87 m at the top, with a total mass of 249,718 kg. The center of mass is located at 43.4 m above SWL.

Mooring lines. The mooring system consists of three catenary mooring lines, each spaced 120° apart. The lines are anchored at a depth of 320 m below SWL, with fairleads positioned 70 m below SWL and a radial distance of 5.2 m from the platform centerline. Each mooring line has an unstretched length of 902.2 m and a diameter of 0.09 m. The equivalent mass density is 77.71 kg/m, while the extensional stiffness is 384.24 MN. The mooring system is modeled to analyze the effect of VIV-induced oscillations on mooring line tension and fatigue.

Blade. The wind turbine blades have a length of 61.5 m and a total mass of 17,740 kg. The aerodynamic profile follows standard NREL airfoils. While the blades are included in the simulation, VIV-induced aerodynamic effects, such as tower shadow and unsteady wake interactions, are not considered.

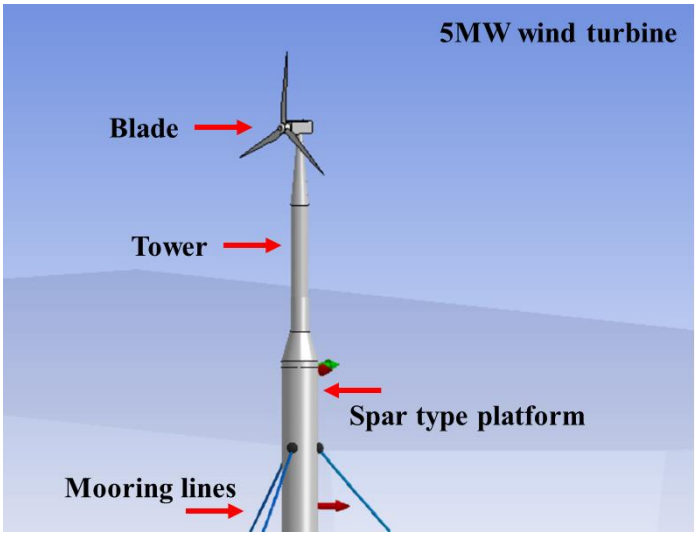

Fig. 1. Schematic representation of the wind turbine model.

Activated Solvers

To ensure accurate numerical simulation of the 5MW Floating Offshore Wind Turbine (FOWT), multiple solver in OpenFAST are used to handle different aspects of the system, such as structural dynamics, hydrodynamics, aerodynamics, and mooring interactions. Table 1 summarizes the feature solvers used in this study, followed by an explanation of their roles in the simulation setup.

Table 1. Activated solvers in OpenFAST simulation.

Solver	Description
ElastoDyn	Models the tower and platform structural dynamics
AeroDyn	Computes aerodynamic loads on the blades (VIV-induced aerodynamic effects excluded)
SeaState	Models current conditions
HydroDyn	Computes hydrodynamic loads. This study includes a modified Morison equation with VIV effects
MoorDyn	Models mooring system forces and interactions

The ElastoDyn module is activated to model the flexible response of the

tower and platform under external loads. The AeroDyn module is activated to compute standard aerodynamic forces on the blades; however, unsteady aerodynamic effects caused by VIV are excluded to isolate hydrodynamic interactions. The SeaState module is used to define current conditions, including current speed, profile, and direction. The HydroDyn module is the primary hydrodynamic solver, responsible for wave loads, added mass, and damping effects. This study modifies the Morison equation within HydroDyn to incorporate VIV-induced forces, allowing for a more accurate representation of platform and mooring line oscillations due to vortex shedding. Finally, the MoorDyn module is used for mooring system modeling, simulating catenary mooring lines that stabilize the platform.

Modified Morison Equation including VIV Effects

The standard Morison equation in HydroDyn accounts for inertia, drag, buoyancy, marine growth effects, and added mass but does not consider VIV. To address this limitation, the present study introduces an additional lift force term based on the vortex shedding frequency (Blevins, 2009):

$$F_y = (1/2)\rho U^2 D L C_L \sin(2\pi f_s t + \varphi) \quad (Unit: N) \tag{1}$$

where ρ is the water density (1050 kg/m^3), U is the free-stream velocity, D is the platform diameter (6.5 m), L is the total draft (120 m), C_L is the lift coefficient, f_s is the vortex shedding frequency, and φ is the phase shift (0 deg). This modification enables a more realistic representation of hydrodynamic forces acting on the platform and mooring system. Eq. 1 is valid within a Reynolds number range of approximately 10,000 to 500,000. With this additional lift force, the modified Morison equation applied along the length of a member is expressed as (Jonkman et al., 2014):

$$F = F_I + F_D + F_B + F_{MG} + F_{F\_B} + F_{AM\_M} + F_{AM\_G} + F_{AM\_F} + F_y \tag{2}$$

where F_I is the inertia force, F_D is the drag force, and F_B is the buoyancy force. F_{MG} represents the weight of marine growth, while F_{F_B} accounts for fluid ballasting effects. The added mass forces include F_{AM_M} for the structure, F_{AM_G} for marine growth, and F_{AM_F} for fluid ballasting. Finally, F_y is the VIV-induced lift force introduced in this study.

Strouhal Number and Vortex Shedding Frequency. The Strouhal number (St) is a dimensionless parameter that relates the vortex shedding frequency (f_s) to the freestream velocity (U) and the characteristic cylinder diameter (D) (Roshko, 1954):

$$f_s = (St)\, {}^{U}/_{D} \tag{3}$$

For Reynolds numbers (Re) below 5×10^5, the Strouhal number varies as a function of Reynolds number. However, for Re > 5×10^5, the Strouhal number stabilizes and becomes nearly independent of Reynolds number (Shih et al., 1993; Zan and Matsuda, 2002). Empirical data suggest that for rough-surface stationary cylinders in this high Re regime, St remains approximately constant at (Shih et al., 1993; Zan and Matsuda, 2002; Roshko, 1954):

$$St = 0.22, \quad 10^5 < Re < 10^7 \tag{4}$$

In this study, the Reynolds number is calculated using the characteristic platform diameter (D = 6.5 m), water kinematic viscosity, and the free stream velocity considered. Even at the lowest velocity, the resulting Re remains greater than 10^5, confirming that the assumption of St = 0.22 is valid for all cases in this study.

Constant Lift Coefficient Model. A stationary circular cylinder in uniform cross-flow typically experiences zero net lift due to symmetric vortex shedding. However, under VIV or forced oscillation, periodic lift forces develop, resulting in a nonzero mean lift coefficient. Blevins (2009) presents a model where the transverse motion of a spring-supported circular cylinder undergoing VIV can be expressed as

$$m\ddot{y} + 2m\zeta_n\omega_n\dot{y} + ky = F_y \tag{5}$$

where m represents the mass of the cylinder, and y denotes its transverse displacement. The term ζ_n corresponds to the damping ratio, while ω_n is the natural frequency of the system. The parameter k represents the structural stiffness, and F_y is the periodic lift force exerted by the fluid on the cylinder as shown in Eq. 1. For high Reynolds number flows (greater than 5×10^5), Blevins (2009) states that a constant lift coefficient of C_L = 1.0 is a reasonable approximation when the Strouhal number is 0.22. Since the Strouhal number in this study is 0.22, adopting C_L = 1.0 ensures consistency with empirical results for oscillating circular cylinders in VIV.

Hydrodynamic Model Discretization and Boundary Conditions

Spatial Discretization of the Spar Platform. The platform is discretized along its vertical axis into multiple segments, ensuring a higher resolution near the free surface where wave-induced forces are most significant. The structure is divided into three primary members, defined by four joints positioned at −120 m, −12 m, −4 m, and 10 m relative to the still water level (SWL). Each member is further subdivided into smaller segments at 0.5 m intervals, resulting in a total of 244 discrete elements. Hydrodynamic forces, including inertial loads, drag, and buoyancy, are computed at each node along these segments using the strip-theory-based Morison equation. The modified Morison equation incorporates vortex-induced vibrations, applying additional force components at each node to account for vortex shedding effects.

Computational Domain Setup. The hydrodynamic simulation is configured within a computational domain that ensures realistic far-field wave propagation and current flow. The total water depth of the simulation is 130 m, providing sufficient clearance beneath the spar platform. The lateral extents of the domain are 30 m in both the X and Y directions, representing an open-sea environment where external forces develop naturally before interacting with the structure. The vertical range spans from −130 m (seabed) to 10 m above SWL. While this domain is sufficient for hydrodynamic simulation, the full aerodynamic simulation accounts for the entire FOWT system, including the blades, reaching up to 126 m.

Current Boundary Condition. The current is applied at the far-field boundary and flows in the positive X-direction toward the platform. It originates at X = –30 m and is modeled as a constant sub-surface current, maintaining the same velocity throughout the water column. This simplification allows for a clear analysis of vortex-induced vibration (VIV) effects without introducing vertical variations in current profile. The applied current speeds at the still water level (SWL) are 0.02 m/s, 0.04 m/s, 0.06 m/s, and 0.08 m/s. The current direction is aligned with the platform's surge axis (X-direction), and it remains steady over time. As a result, hydrodynamic forces such as drag, inertia, and VIV-induced lift act on the submerged sections of the spar platform. This uniform current profile is suitable for isolating the influence of current-induced forces on the floating structure dynamics.

Global Coordinate System and Degrees of Freedom in Floating Offshore Wind Turbine Dynamics. Fig. 2 illustrates the global coordinate system and the six degrees of freedom (DOF) governing the

dynamic response of the floating offshore wind turbine (FOWT). The origin of this coordinate system is defined at the center of the spar platform, which is located 10 meters below the still water level, along the central vertical axis of the structure. The X-axis extends downwind, aligning with the primary wind direction, while the Y-axis is oriented perpendicular to the wind direction, defining the lateral direction. The Z-axis points upward, corresponding to the tower and rotor height. The FOWT experiences six degrees of freedom (DOF), encompassing three translational and three rotational motions. The translational motions include surge (X-direction, forward-backward motion), sway (Y-direction, side-to-side motion), and heave (Z-direction, vertical displacement). The rotational motions consist of roll (rotation about the X-axis), pitch (rotation about the Y-axis), and yaw (rotation about the Z-axis). These movements result from interactions with environmental forces such as wind, waves, and currents, affecting both the structure and mooring system.

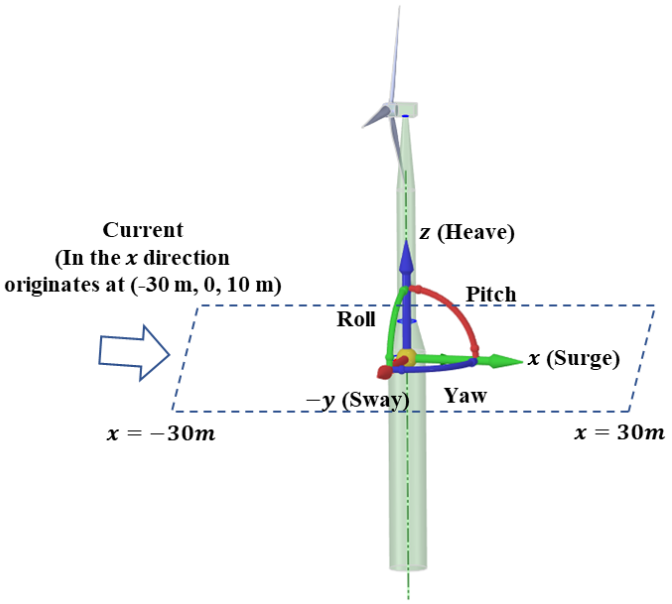

Fig. 2. Global coordinate system and six degrees of freedom of turbine.

Simulation Setup

The numerical simulation was performed over a total duration of 20,000 seconds using a time step of 0.025 s, chosen to ensure a balance between computational efficiency and solution accuracy. To verify the adequacy of this choice, a time-step sensitivity analysis was conducted at the highest current speed of 0.08 m/s, comparing simulation results obtained with $\Delta t = 0.0250$ s and $\Delta t = 0.0125$ s over a 1-hour period. As shown in Fig. 3, both cases yield nearly identical time histories of the y-directional hydrodynamic force, confirming that $\Delta t = 0.025$ s is sufficiently accurate for capturing the platform's dynamic response under steady current conditions. To focus on the effects of VIV under steady conditions, this study focuses solely on the influence of steady ocean currents. Unlike previous configurations that considered separate cases involving waves, wind, and currents, the current analysis systematically varies the current speed at 0.02, 0.04, 0.06, and 0.08 m/s, while excluding both wave and wind effects. This steady-state framework aligns with the assumptions used in the derivation of Eq. 1, which models VIV-induced lift forces. Furthermore, these current speeds correspond to Reynolds numbers of approximately 130,000, 260,000, 390,000, and 520,000, respectively falling within the valid range for applying Eq. 1 as proposed by Blevins (2009).

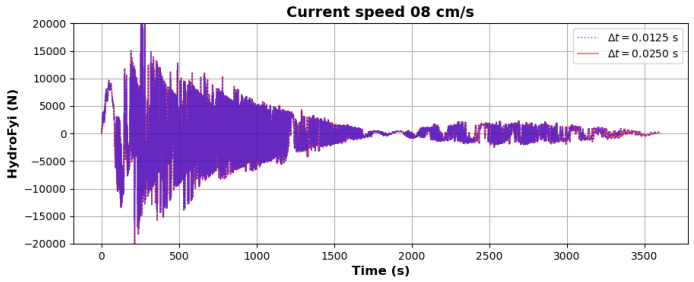

Fig. 3. Time-step sensitivity analysis of y-directional hydrodynamic force (HydroFyi) at 0.08 m/s steady current speed.

RESULTS

To assess the influence of vortex-induced vibration (VIV) modeling, two simulation cases were defined. Case 1 assumes a stationary platform, using the steady current velocity as the free-stream velocity without feedback from platform motion. This case focuses solely on the hydrodynamic force without structural feedback, allowing for direct validation against analytical predictions. Case 2 incorporates platform motion by using the relative velocity, allowing two-way coupling between the VIV-induced force and structural response. This setup captures realistic platform dynamics. Comparing these cases highlights the importance of coupling effects in accurate VIV modeling.

Case 1: Stationary platform

VIV-induced lift force. In this case, the platform is assumed to be fixed in space, with no motion feedback to the fluid domain. Table 2 presents the analytically computed VIV-induced lift forces and corresponding vortex shedding frequencies at various steady current speeds. These values are obtained using Eq. 1, which defines the sinusoidal lift force induced by vortex shedding, and Eq. 3, which relates the vortex shedding frequency to the free-stream velocity via the Strouhal number. The table highlights that both the lift force magnitude and shedding frequency increase with current speed, consistent with expected VIV behavior in the Reynolds number range of 10^4 to 5×10^5 where the adopted lift coefficient formulation is known to be valid. This table serves as the reference baseline for evaluating the numerical results presented in Fig. 4 and Fig. 5.

Table 2. Computed VIV-induced lift forces and corresponding vortex shedding frequencies for various steady current speeds.

Current speed	VIV-induced lift force	Vortex shedding frequency
0.02 m/s	163.8 N	0.000677 Hz
0.04 m/s	655.2 N	0.001354 Hz
0.06 m/s	1474.2 N	0.002031 Hz
0.08 m/s	2620.8 N	0.002708 Hz

Fig. 4 illustrates the time-domain evolution of the y-directional hydrodynamic force (HydroFyi), which corresponds to the lift force acting on the platform origin due to VIV, for four different steady current speeds (0.02, 0.04, 0.06, and 0.08 m/s). Two modeling cases are compared: the conventional Morison equation without VIV (blue lines) and the modified version including the VIV-induced lift term (red lines). As shown, the conventional case results in near-zero force with negligible fluctuations, while the VIV-modified case exhibits clear oscillatory behavior whose amplitude increases with current speed. These oscillations are direct evidence of vortex shedding behind the

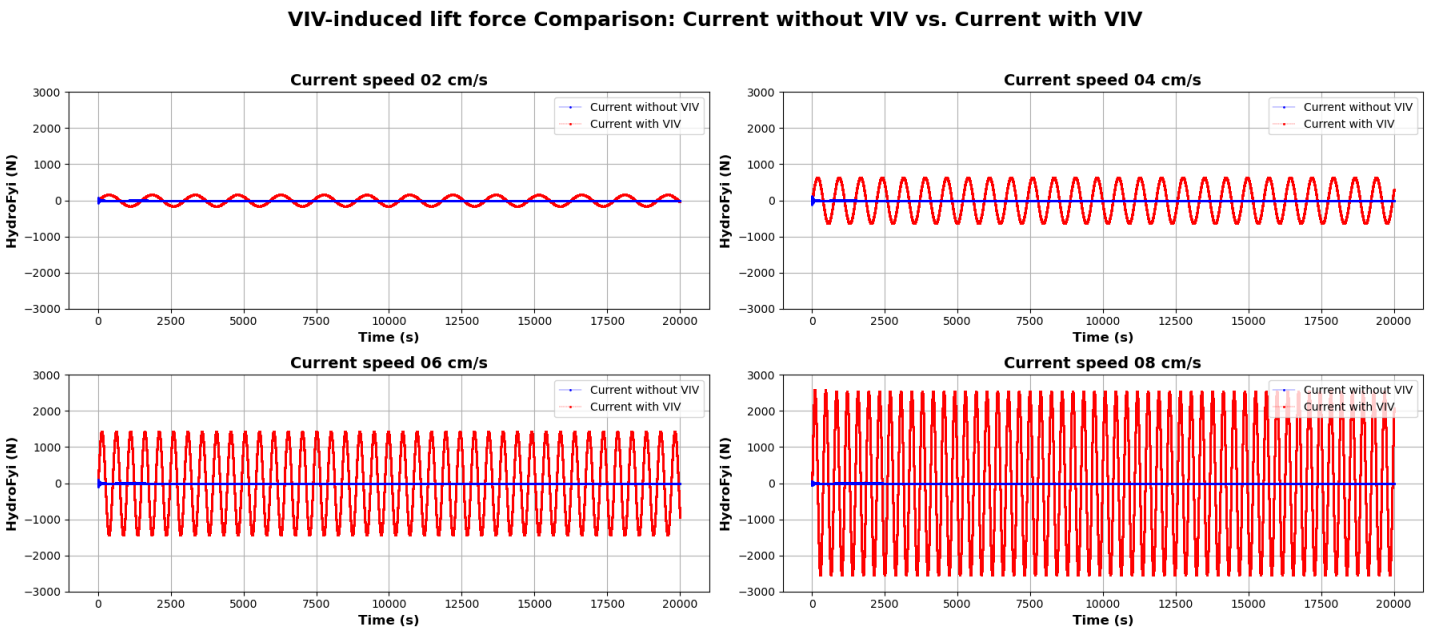

Fig. 4. Time-domain comparison of VIV-induced lift forces with and without VIV Effects for various steady current speeds (Stationary platform).

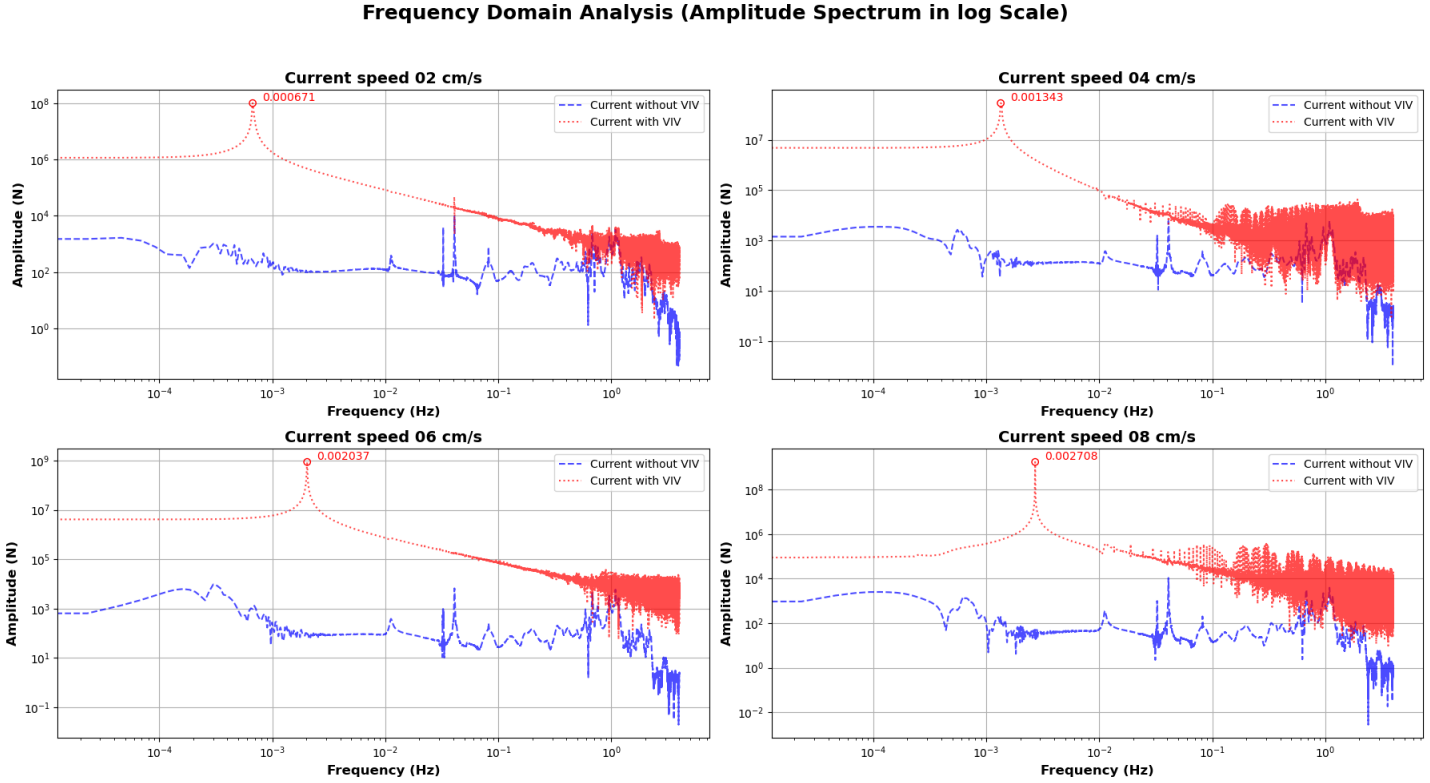

Fig. 5. Frequency-domain analysis of VIV-induced lift forces: amplitude spectra showing vortex shedding peaks (Stationary platform).

platform and validate the physical representation introduced in the modified model. The amplitude of the oscillating force grows proportionally with current speed, matching closely with the theoretical lift force values in Table 2. For instance, the peak-to-peak variations in the time series at 0.08 m/s correspond well with the predicted lift force of 2620.8 N, verifying the correct implementation of the lift force formulation within HydroDyn. To complement the time-domain validation, Fig. 5 presents the corresponding frequency-domain spectra, obtained through Fast Fourier Transform (FFT) of the HydroFyi signal. In each VIV case, a distinct spectral peak is observed, which aligns almost exactly with the analytically computed vortex shedding frequency from Table 2 (e.g., 0.002708 Hz for 0.08 m/s). These peaks

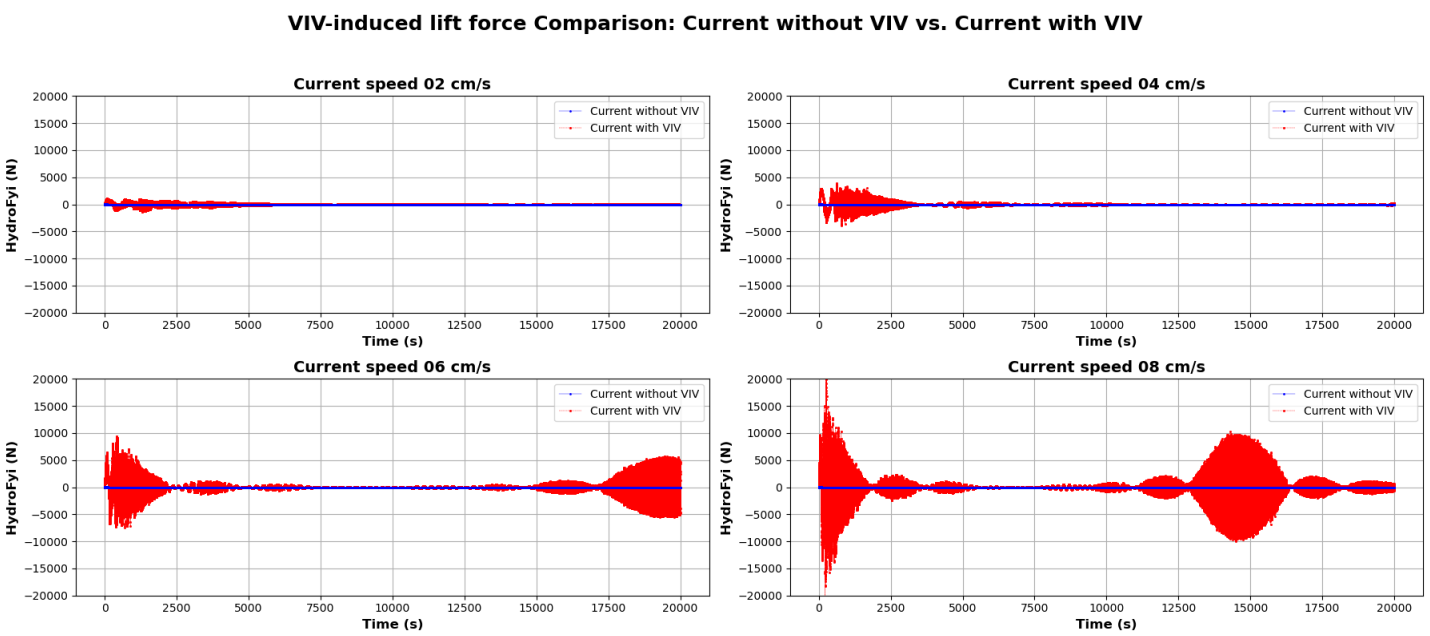

Fig. 6. Time-domain response of platform sway (y-direction) under steady current conditions with and without VIV (Moving platform).

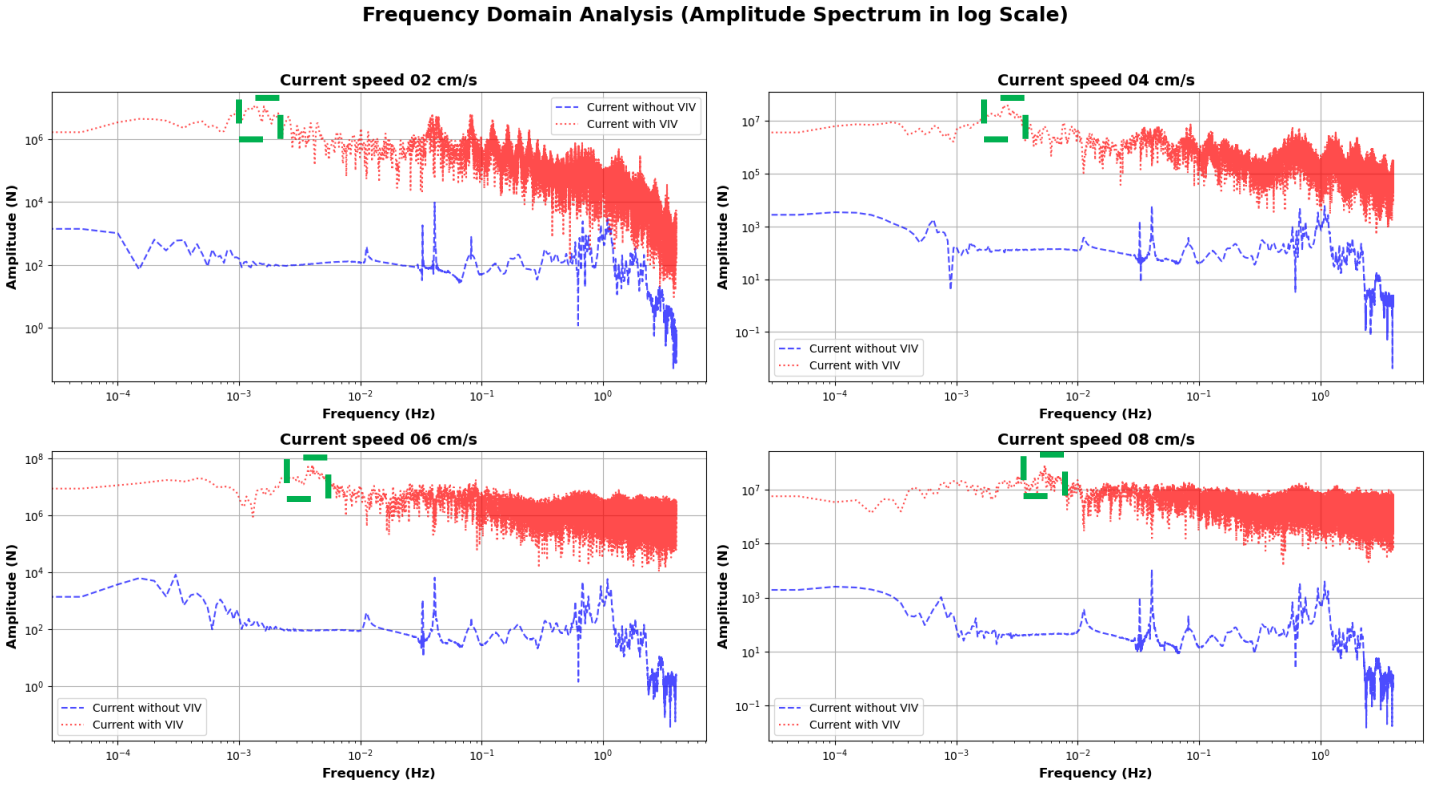

Fig. 7. Frequency-domain analysis of VIV-induced lift forces: amplitude spectra showing vortex shedding peaks (Moving platform).

are absent in the no-VIV cases, further confirming that the oscillatory forces stem from the modeled vortex-induced effects. Together, Table 2 and Fig. 4, 5 confirm the effectiveness of the modified Morison equation in capturing both the magnitude and frequency content of lift forces arising from vortex shedding. These findings underscore the necessity of incorporating VIV-induced forces in the hydrodynamic modeling of floating offshore wind turbines, especially under steady current conditions where such effects become dynamically significant.

Case 2: Moving platform

VIV-induced lift force. Fig. 6 displays the time-domain history of the y-

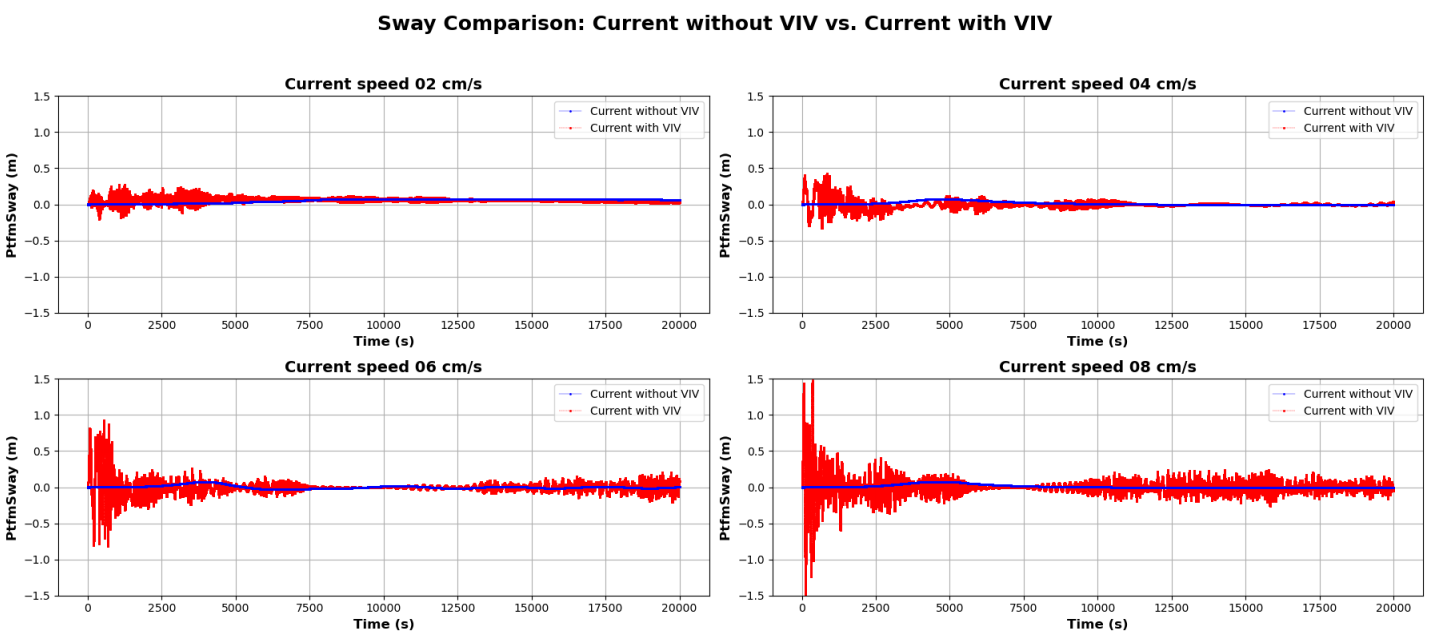

Fig. 8. Time-domain response of platform sway (y-direction) under steady current conditions with and without VIV (Moving platform).

directional hydrodynamic force (HydroFyi) acting on the floating platform under steady currents of 0.02 ~ 0.08 m/s. Unlike the stationary case (Fig. 4), where a single vortex shedding frequency dominates, the inclusion of platform motion introduces varying relative velocities across structural members, leading to the superposition of multiple shedding frequencies. At higher current speeds, the lift force exhibits constructive and destructive interference patterns, producing beating-like oscillations with alternating amplitude growth and decay. This complex force behavior results from two-way coupling between the flow and platform motion. The corresponding frequency spectra in Fig. 7 reveal multiple peaks of comparable amplitude across the low-frequency band (highlighted by the green dashed box), confirming the presence of overlapping VIV modes rather than a single dominant frequency. An initial spike in force is observed across all cases, caused by platform oscillation due to the rotor-nacelle's upstream mass. As current speed increases, the amplitude of the VIV-induced force grows nonlinearly, consistent with the square-law dependency in Eq. 1. These results emphasize the importance of including platform motion to realistically capture VIV forces in floating wind turbine modeling.

Overall, the results from Case 2 confirm that incorporating platform motion through the use of relative velocity fundamentally changes the nature of the hydrodynamic force. The lift force becomes richer in frequency content and larger in amplitude, especially at higher flow velocities, indicating that simplified assumptions based on steady or uniform flow may substantially underestimate the true dynamic loading on the structure. These findings highlight the need for VIV models that account for two-way coupling in order to capture the realistic behavior of floating offshore wind turbines under current-dominated conditions.

Platform sway response. Fig. 8 illustrates the platform sway (PtfmSway) response for varying current speeds, comparing simulations with and without VIV effects. In the absence of VIV, lateral motion remains minimal due to the lack of unsteady lift forces. With VIV, however, significant sway oscillations develop, increasing in both amplitude and complexity with current speed. The sway response closely follows the behavior of the lift force, reflecting strong coupling between fluid forces and platform motion. At low speeds, the sway shows low-amplitude, asymmetric oscillations, while higher speeds induce pronounced beating patterns due to interference among multiple VIV modes. These results confirm that VIV can drive large sway displacements, exceeding 1.0 m at 0.08 m/s, which may contribute to fatigue or mooring system stress. Accurate modeling of such effects is essential for reliable FOWT design under steady current conditions.

DISCUSSIONS

Future Considerations

Need for Validation through CFD or Experiments. Although this study provides a detailed numerical analysis of VIV effects on floating offshore wind platforms, experimental validation was not performed due to the lack of matching physical data. The OC3 spar platform, used here as a numerical benchmark developed by NREL, has not been tested under isolated current-only conditions at prototype scale. While scaled model tests exist in literature, they typically involve different platform designs or combined environmental conditions, limiting their applicability for direct comparison. To overcome this, future work will employ high-fidelity CFD simulations using OpenFOAM to directly capture vortex shedding and its interaction with platform motion. These simulations will serve both as a validation tool for the modified HydroDyn model and as a means to improve understanding of VIV phenomena beyond empirical force formulations.

Space discretization considerations. The platform was discretized at 0.5-meter intervals along its vertical axis, following standard practices for Morison-based hydrodynamic modeling. This resolution is considered sufficient for the stationary platform case under a constant current profile, where force distribution remains relatively uniform. However, in the moving platform case, relative velocity varies with structural motion, potentially introducing localized force fluctuations. To address this, future work will explore mesh sensitivity by refining the spatial discretization, ensuring accurate force prediction in dynamically coupled simulations.

Need for Implementing VIV Effects in AeroDyn. The current study clearly demonstrates that VIV can significantly alter the hydrodynamic forces and platform response under current-dominated conditions when properly implemented through relative velocity formulations in HydroDyn. However, these VIV effects are not yet represented in the aerodynamic module AeroDyn, which governs wind-induced loading on the rotor, nacelle, and tower components. As a result, potential VIV effects driven by aerodynamic forces are currently unmodeled. This omission may lead to underestimation of unsteady aerodynamic loading, especially in scenarios involving steady wind flow around the tower where vortex shedding is likely. To improve predictive capability, future versions of AeroDyn should consider incorporating unsteady aerodynamic force components arising from vortex shedding, similar to the modifications applied in HydroDyn. In particular, the influence of tower shadow effects, where periodic shedding can alter the incoming velocity field experienced by the blades, should be addressed. Failure to include these variations could lead to inaccuracies in blade loading prediction and structural fatigue assessment.

Implementation of VIV Effects in a Hybrid Hydrodynamic model. Currently, HydroDyn accounts for hydrodynamic forces using only the Morison equation, which is primarily suited for slender structures where inertia and drag forces dominate. However, for floating platforms, potential flow effects also play a crucial role in capturing radiation and diffraction forces. A hybrid model that combines Morison's equation with potential flow theory would provide a more comprehensive representation of hydrodynamic loading. Incorporating VIV effects into such a hybrid model is essential, as vortex shedding can interact with wave radiation forces, influencing platform motions more significantly than in a purely Morison-based approach.

CONCLUSIONS

This study presents a modified OpenFAST framework that incorporates vortex-induced vibration (VIV) effects into the hydrodynamic force calculations of floating offshore wind turbines (FOWTs) through an additional lift force term in the Morison equation. Simulations were performed under steady current conditions using the OC3 spar-type platform to isolate and evaluate the influence of VIV on both hydrodynamic forces and platform motion. The results demonstrate that when platform motion is neglected, the lift force follows a single-frequency oscillation governed by vortex shedding, which agrees well with analytical predictions. However, when relative velocity is considered, the platform exhibits complex, multi-frequency force responses due to the superposition of vortex shedding across different members. This dynamic coupling results in amplified force and sway oscillations, particularly at higher current speeds, which would be missed in conventional models. The platform sway motion reaches amplitudes over 1.0 m at 0.08 m/s, revealing the potential significance of VIV on structural fatigue and mooring system performance. The findings confirm that incorporating VIV into hydrodynamic modeling is essential for capturing realistic platform dynamics. While prototype-scale validation data for current-only conditions remain unavailable, future work will involve CFD simulations using OpenFOAM to resolve vortex shedding behavior and support model accuracy. In addition, expanding VIV modeling into the aerodynamic module AeroDyn, and exploring hybrid hydrodynamic models and multi-directional flow scenarios, will further improve the fidelity of FOWT simulations under real ocean conditions.

ACKNOWLEDGEMENT

This work was supported by a grant from the Michigan Institute for Computational Discovery and Engineering (MICDE)

REFERENCES

Blevins, RD (2009). "Models for Vortex-Induced Vibration of Cylinders Based on Measured Forces," *J Fluids Eng*, 131(10), 101203.

Chen, J, Hu, Z, Liu, G, and Wan, D (2019). "Coupled Aero-Hydro-Servo-Elastic Methods for Floating Wind Turbines," *Renew Energy*, 130, 139-153.

Facchinetti, ML, De Langre, E, and Biolley, F (2004). "Coupling of Structure and Wake Oscillators in Vortex-Induced Vibrations," *J Fluids Struct*, 19(2), 123-140.

Gabbai, RD, and Benaroya, H (2005). "An Overview of Modeling and Experiments of Vortex-Induced Vibration of Circular Cylinders," *J Sound Vib*, 282(3-5), 575-616.

Jonkman, JM, and Buhl, ML (2005). *FAST User's Guide*, NREL/TP-500-38230, National Renewable Energy Laboratory, Golden, CO.

Jonkman, J, Butterfield, S, Musial, W, and Scott, G (2009). *Definition of a 5-MW Reference Wind Turbine for Offshore System Development*, NREL/TP-500-3823, National Renewable Energy Laboratory, Golden, CO.

Jonkman, JM (2010). *Definition of the Floating System for Phase IV of OC3*, NREL/TP-500-47535, National Renewable Energy Laboratory, Golden, CO.

Jonkman, JM, Robertson, AN, and Hayman, GJ (2014). *HydroDyn User's Guide and Theory Manual*, National Renewable Energy Laboratory, Golden, CO.

Morison, JR, Johnson, JW, and Schaaf, SA (1950). "The Force Exerted by Surface Waves on Piles," *J Petrol Technol*, 2(5), 149-154.

Putri, RM, Obhrai, C, Jakobsen, JB, and Ong, MC (2020). "Numerical Analysis of the Effect of Offshore Turbulent Wind Inflow on the Response of a Spar Wind Turbine," *Energies*, 13(10), 2506.

Roshko, A. (1954). *On the drag and shedding frequency of two-dimensional bluff bodies* (No. NACA-TN-3169). National Advisory Committee for Aeronautics.

Shih, WCL, Wang, C, Coles, D, and Roshko, A (1993). "Experiments on Flow Past Rough Circular Cylinders at Large Reynolds Numbers," *J Wind Eng Ind Aerodyn*, 49, 351–368.

Sumer, BM (2006). *Hydrodynamics Around Cylindrical Structures*, World Scientific, 26.

Tran, TT, and Kim, DH (2015). "The Aerodynamic Interference Effects of a Floating Offshore Wind Turbine Experiencing Platform Pitching and Yawing Motions," *J Mech Sci Technol*, 29, 549-561.

Tran, TT, and Kim, DH (2016). "A CFD Study into the Influence of Unsteady Aerodynamic Interference on Wind Turbine Surge Motion," *Renew Energy*, 90, 204-228.

Williamson, CH, and Govardhan, R (2004). "Vortex-Induced Vibrations," *Annu Rev Fluid Mech*, 36(1), 413-455.

Zan, SJ, and Matsuda, K (2002). "Steady and Unsteady Loading on a Roughened Circular Cylinder at Reynolds Numbers up to 900,000," *J Wind Eng Ind Aerodyn*, 90, 567–581.

Zhang, W, Calderon-Sanchez, J, Duque, D, and Souto-Iglesias, A (2024). "Computational Fluid Dynamics (CFD) Applications in Floating Offshore Wind Turbine (FOWT) Dynamics: A Review," *Appl Ocean Res*, 150, 104075.

Zhong, W, Wang, N, and Wan, D (2022). "A Coupled CFD and Dynamic Mooring Model for FOWT Hydrodynamics," *Proc ISOPE Int Ocean and Polar Eng Conf*, ISOPE-I, ISOPE.